Human lung-resident macrophages express CB₁ and CB₂ receptors whose activation inhibits the release of angiogenic and lymphangiogenic factors

Rosaria I. Staiano,[*,1] *Stefania Loffredo,*[*,1] *Francesco Borriello,*[*] *Fabio Arturo Iannotti,*[†]
Fabiana Piscitelli,[†] *Pierangelo Orlando,*[‡] *Agnese Secondo,*[§] *Francescopaolo Granata,*[*]
Maria Teresa Lepore,[*] *Alfonso Fiorelli,*[¶] *Gilda Varricchi,*[*] *Mario Santini,*[¶] *Massimo Triggiani,*[‖]
Vincenzo Di Marzo,[†,2] *and Gianni Marone*[*,#,2]

Departments of *Translational Medical Sciences and Center for Basic and Clinical Immunology Research and §Neuroscience,
Reproductive and Odontostomatological Sciences, University of Naples Federico II, Naples, Italy; †Endocannabinoid Research
Group, Institute of Biomolecular Chemistry, Consiglio Nazionale delle Ricerche, Pozzuoli, Naples, Italy; ‡Endocannabinoid
Research Group, Institute of Protein Biochemistry, Consiglio Nazionale delle Ricerche, Naples, Italy; ¶Thoracic Surgery Unit,
Second University of Naples, Naples, Italy; ‖Division of Allergy and Clinical Immunology, University of Salerno, Salerno, Italy; and
#Consiglio Nazionale delle Ricerche Institute of Experimental Endocrinology and Oncology "G. Salvatore," Naples, Italy

ABSTRACT

Macrophages are pivotal effector cells in immune responses and tissue remodeling by producing a wide spectrum of mediators, including angiogenic and lymphangiogenic factors. Activation of cannabinoid receptor types 1 and 2 has been suggested as a new strategy to modulate angiogenesis in vitro and in vivo. We investigated whether human lung-resident macrophages express a complete endocannabinoid system by assessing their production of endocannabinoids and expression of cannabinoid receptors. Unstimulated human lung macrophage produce 2-arachidonoylglycerol, N-arachidonoyl-ethanolamine, N-palmitoyl-ethanolamine, and N-oleoyl-ethanolamine. On LPS stimulation, human lung macrophages selectively synthesize 2-arachidonoylglycerol in a calcium-dependent manner. Human lung macrophages express cannabinoid receptor types 1 and 2, and their activation induces ERK1/2 phosphorylation and reactive oxygen species generation. Cannabinoid receptor activation by the specific synthetic agonists ACEA and JWH-133 (but not the endogenous agonist 2-arachidonoylglycerol) markedly inhibits LPS-induced production of vascular endothelial growth factor-A, vascular endothelial growth factor-C, and angiopoietins and modestly affects IL-6 secretion.

No significant modulation of TNF-α or IL-8/CXCL8 release was observed. The production of vascular endothelial growth factor-A by human monocyte-derived macrophages is not modulated by activation of cannabinoid receptor types 1 and 2. Given the prominent role of macrophage-assisted vascular remodeling in many tumors, we identified the expression of cannabinoid receptors in lung cancer-associated macrophages. Our results demonstrate that cannabinoid receptor activation selectively inhibits the release of angiogenic and lymphangiogenic factors from human lung macrophage but not from monocyte-derived macrophages. Activation of cannabinoid receptors on tissue-resident macrophages might be a novel strategy to modulate macrophage-assisted vascular remodeling in cancer and chronic inflammation. *J. Leukoc. Biol.* 99: 531–540; 2016.

Abbreviations: AA = arachidonic acid, ABHD = α,β-hydrolase domain, ABHD6 = ABHD containing 6, ABHD12 = ABHD containing 12, AEA = anandamide, 2-AG = 2-arachidonoylglycerol, Fura-AM = Fura-acetoxymethyl ester, Ang1 = angiopoietin 1, Ang2 = angiopoietin 2, $[Ca^{2+}]i$ = intracellular calcium concentration, CB_1 = cannabinoid receptor type 1, CB_2 = cannabinoid receptor type 2, DAG = 1,2-diacylglycerol,

(continued on next page)

The online version of this paper, found at www.jleukbio.org, includes supplemental information.

Introduction

Macrophages are implicated in such pathologic processes as chronic inflammation, tissue remodeling, and tumor growth because of their ability to produce proinflammatory mediators and angiogenic and lymphangiogenic factors [1–4] in response to a wide spectrum of stimuli [5]. Their activation status can be roughly divided into 2 subgroups, M1 and M2. M1 macrophages are proinflammatory and have a central role in host defense against bacterial infections, and M2 macrophages are associated

with the response to parasitic infections, tissue remodeling, and tumor progression. In addition, tissue-resident macrophages might be functionally different from in vitro-derived macrophages owing to their ontogeny and/or tissue-derived signals [6–10].

ECs are lipid mediators that exert most of their functions by activating two 7-transmembrane G-protein–coupled receptors, CB_1 and CB_2 [11, 12]. ECs, together with their receptors and the proteins responsible for their synthesis, transport, and degradation, constitute the EC system [13]. CB_1 is abundant in the central nervous system, and it is also expressed in the peripheral system [14–16]. CB_2 is primarily found in peripheral tissues, several immune cell subsets [16, 17], and, to a lesser extent, neuronal cells [18]. Specifically, CB_2 has been identified in mouse macrophages [19, 20] and human monocytes [21, 22], and CB_1 has been found in mouse [23] and human monocytes [24] and mast cells [25, 26]. Angiogenesis, the formation of new blood vessels, and lymphangiogenesis, the formation of new lymphatic vessels, are complex processes [27] that require the coordinated action of several factors, including VEGFs and Ang1 and Ang2. Evidence has shown that activation of CB_1 and CB_2 inhibits angiogenesis in vivo and in vitro [28–32]. CB_1 [32] and CB_2 [33] activation reduces the expression of VEGFs in tumors. To our knowledge, no evidence has shown that CB_1 or CB_2 activation modulates human macrophage-assisted vascular remodeling.

In the present study, we investigated the production of ECs, the expression of CB_1 and CB_2 in HLMs, and the effects of CB_1 and CB_2 agonists on the production of angiogenic and lymphangiogenic factors from LPS-activated HLMs.

MATERIALS AND METHODS

Isolation and purification of HLMs and monocytes

HLMs and human blood cells were obtained according to the human subject research guidelines established by the University of Naples Federico II and the Second University of Naples. The ethics committee of the University of Naples Federico II approved the study protocol, and patients undergoing thoracic surgery and blood donors provided informed consent.

Macroscopically normal lung tissue was obtained from patients affected by lung adenocarcinoma (hepatitis C virus-negative, hepatitis B surface Ag-negative, HIV1$^-$) undergoing lung resection, and HLMs were isolated by mechanical dispersion, as previously described [34].

For monocyte isolation, blood was layered onto Histopaque-1077 (Sigma-Aldrich, Milan, Italy), and mononuclear cells were collected at the interface. Monocytes were further purified with CD14 microbeads (Miltenyi Biotec, Bologna, Italy) according to the manufacturer's protocol.

Cell cultures

Cells were cultured in 24-well plates in RPMI 1640 supplemented with 5% FCS (Sigma-Aldrich), 2 mM L-glutamine, and 1% antibiotic-antimycotic solution.

(continued from previous page)

DAGLα = diacylglycerol lipase α, DAGLβ = diacylglycerol lipase β, EC = endocannabinoid, FAAH = fatty acid amide hydrolase, HLM = human lung macrophage, MAGL = monoacylglycerol lipase, MDM = monocyte-derived macrophage, OEA = N-oleoyl-ethanolamine, PCG = PIPES calcium glucose, PEA = N-palmitoyl-ethanolamine, PLCβ = phospholipase Cβ1 (phosphoinositide-specific), ROS = reactive oxygen species, VEGF = vascular endothelial growth factor

To obtain MDMs, monocytes (2×10^5 cells/cm^2) were differentiated with M-CSF 50 ng/ml (Miltenyi Biotec) for 7 d.

The cells were treated with different combinations of vehicle (DMSO, also reported as untreated), ACEA (CB_1 agonist; Tocris Bioscience, Bristol, U.K.), JWH-133 (CB_2 agonist; Tocris Bioscience), detoxified LPS (from *Escherichia coli* serotype 0111:B4; Sigma-Aldrich), AM-251 (CB_1 antagonist; Tocris Bioscience), AM-630 (CB_2 antagonist; Tocris Bioscience), OMDM-169 (an inhibitor of 2-AG degradation), OMDM-188 (an inhibitor of 2-AG synthesis), EGTA (Sigma-Aldrich), and BAPTA (Sigma-Aldrich). At the end of incubation, the supernatants were collected and stored at −80°C for subsequent ELISA quantification. The remaining cells were lysed with 0.1% Triton X-100 (Sigma-Aldrich) for total protein quantification using a Bradford-based assay (Bio-Rad, Segrate, Italy). Stock solutions of glycolipid were prepared and stored in DMSO at a concentration of 1 M, unless otherwise specified, and diluted to a working concentration in RPMI 1640 or PCG buffer immediately before the experiment.

Quantitative analysis of ECs and related mediators

Freshly isolated HLMs were suspended in PCG buffer. The cells ($5 \times 10^6/2.5$ ml per sample) were incubated (5–360 min, 37°C) with or without 1 µg/ml LPS. Next, 5 ml of ice-cold methanol was added to the cell suspensions, vortexed, and frozen to −80°C. Lipids were extracted from the cell suspensions and AEA, 2-AG, PEA, and OEA prepurified and quantified by isotope dilution-liquid chromatography-atmospheric pressure chemical ionization-mass spectrometry. The extraction, purification, and quantification of ECs from tissues were performed as previously described [35, 36].

Intracellular calcium concentrations

$[Ca^{2+}]i$ was measured by single-cell computer-assisted video imaging [37]. In brief, HLMs cultured on poly-L-lysine–coated glass coverslips were loaded with 6 µM Fura-2 AM for 1 h at 22°C in Krebs-Ringer saline solution containing the following: 5.5 mM KCl, 160 mM NaCl, 1.2 mM MgCl$_2$, 1.5 mM CaCl$_2$, 10 mM glucose, and 10 mM HEPES-NaOH (pH 7.4). At the end of the loading period, the coverslips were placed in a perfusion chamber (Medical Systems, Greenvale, NY, USA) mounted on a Zeiss Axiovert 200 microscope (Carl Zeiss, Jena, Germany) equipped with a FLUAR ×40 oil objective lens. The experiments used a digital imaging system composed of a MicroMax 512BFT cooled charge-coupled device camera (Princeton Instruments, Trenton, NJ, USA), LAMBDA 10-2 filter wheeler (Sutter Instruments, Novato, CA, USA), and MetaMorph/MetaFluor Imaging System software (Universal Imaging, West Chester, PA, USA). After loading, the cells were illuminated alternately at 340 and 380 nm by a xenon lamp. The emitted light was passed through a 512-nm barrier filter. The Fura-2 AM fluorescence intensity was measured every 3 s. A total of 40–65 individual cells were selected and monitored simultaneously from each cover slip. The results are presented as the cytosolic $[Ca^{2+}]$. Calibrations used the relation of Grynkiewicz et al [38], assuming that the K_D for Fura-2 AM was 224 nM.

mRNA extraction and quantitative PCR analysis

Total RNA was isolated using TRI-Reagent (Life Technologies, Monza, Italy) and treated with DNase-I (1 U/µl; Sigma-Aldrich) following the manufacturer's instructions. RNA quality and integrity were estimated using the 2100 Agilent Bioanalyzer (Agilent Technologies, Santa Clara, CA, USA). Total mRNA was reverse transcribed (enzyme-VILO; Life Technologies), and quantitative PCR was performed in the iCycler-iQ5 real-time PCR detection system (Bio-Rad) using SYBR Green Master Mix (Bio-Rad). β-*Actin* was used as the housekeeping gene to normalize the cycle threshold values using the $2^{-\Delta Ct}$ formula. The following primer pairs were used: β-*actin* forward, 5′-AAATCGTGCGTGACATTAAG-3′; β-*actin* reverse, 5′-ATGGAGTTGAAGGTA-GTTTCG-3′; *CB1* forward, 5′-TCTGTTCATCGTGTATGC-3′; *CB1* reverse, 5′-CTTGGCTAACCTAATGTCC-3′; *CB2* forward, 5′-TAGTGCTGAGAGGA-CCCA-3′; *CB2* reverse, 5′-CGCTATCCACCTTCCTACAA-3′; *ABHD6* forward, 5′-CTCAGTGTGGTCAAGTTC-3′; *ABHD6* reverse, 5′-ATCCGATGGGTA-GTAAGC-3′; *ABHD12*, forward, 5′-GGTTCTTCCTTGATCCTATTAC-3′; *ABHD12* reverse, 5′- AATGTATTTGTGCCTGTAGC-3′; *DAGLα* forward, 5′-CGAGTTCATCTACGCCATC-3′; *DAGLα* reverse, 5′-AAGACGCAGAGGACAGTG-3′;

DAGLβ forward, 5′-CTGTGGTGGATTGGCATTC-3′; *DAGLβ* reverse, 5′-GGGTTA-CAAATCGTTCCTCTC-3′; *FAAH* forward, 5′-TCAGAGAAGAGGTCTACA-3′; *FAAH* reverse, 5′- GAGGGCATGGTATAGTT-3′; *MAGL* forward, 5′-AAGATGCCGCCTGTA-GCC-3′; *MAGL* reverse, 5′-TGGGTCGCTGCTGGAAGG-3′; *PLCβ1* forward, 5′-AGA-CAATGGACCTGGCTATG-3′; and *PLCβ1* reverse, 5′-ATGCCTTCCTCCTTGTA-TCC-3′.

Western blot for CB_1 and CB_2

For CB_1 and CB_2 detection, HLMs or MDMs were lysed with lysis buffer (20 mmol/L Tris [pH 7.5], 5 mmol/L EDTA, 1 mmol/L phenylmethylsulfonyl fluoride, 2 mmol/L benzamidine, 10 mg/ml leupeptin, 10 mmol/L NaF, 150 mmol/L NaCl, 1% Nonidet P-40, and 5% glycerol) on ice for 20 min before centrifugation (15 min, 15,000*g*). For p-ERK1/2 detection, HLMs or MDMs were incubated (30 min, 37°C) with CB agonists in PCG buffer and then lysed with lysis buffer. Lysates (40 μg for CB_1 and CB_2, 25 μg for p-ERK1/2) were boiled for 5 min in Laemmli SDS loading buffer, separated on precast polyacrylamide gels (4–12% gradient Bis-Tris gels; Life Technologies), and transferred to poly-vinylidene difluoride (CB_1 and CB_2) or nitrocellulose (p-ERK1/2) membranes. The membranes were incubated (16 h, 4°C) with rabbit anti-CB_1 (1:500; Applied Biologic Materials), mouse anti-CB_2 (1:400; Sigma-Aldrich), or rabbit anti–p-ERK1/2 Ab (1:2000; Cell Signaling Technology, The Netherlands). Mouse anti–α-tubulin (1:5000; Sigma-Aldrich) or rabbit anti-ERK2 (Santa Cruz Bio-technology, Santa Cruz, CA, USA) were used to check for equal protein loading. Reactive bands were detected by chemiluminescence. Images were analyzed on a ChemiDoc XRS station with Quantity-one, version 4.6, software (Bio-Rad).

ROS detection

HLMs were plated in a 24-well plate and incubated (30 min, 37°C) with 10 μM C2′,7′-dichlorodihydrofluorescein diacetate (Life Technologies) in PCG buffer, washed twice, and stimulated with ACEA or JWH-133 (1 μM) and AM-251 or AM-630 (0.5 μM). Immediately after stimulation, the cells were placed in a multimode microplate reader (Infinite 200PRO; Tecan Systems, San Jose, CA, USA) at 37°C, and fluorescence was measured for 10 min at 1-min intervals. In selected experiments, HLMs were preincubated 10 min with AM-251 or AM-630 and then stimulated with ACEA or JWH-133.

Immunohistochemistry analysis of nontumor and tumor lung tissues

Nontumor and tumor lung tissues were obtained from patients undergoing resection for lung cancer [34]. The tissues were fixed with 4% para-formaldehyde (wt/vol) paraformaldehyde/PBS. After fixation, lung slices were cut with a Leica CM3050S cryostat (Leica Biosystems, Nussloch, Germany) in serial coronal frozen sections (10 μm thick), collected onto electrostatic-charged Super frost slides (Thermo Scientific, Milan, Italy) in alternate series and processed for immunohistochemistry. The following antibodies were used: mouse anti-CD68 (Thermo Scientific), rabbit anti-CB_1, rabbit anti-CB_2 (Abcam, Cambridge, U.K.), Alexa Fluor-488 or -546 secondary donkey anti-IgGs (Life Technologies). For detection, we used Polink TS-MMR-Hu KIT (GBI Labs, Bothell, WA, USA) and mouse AP polymer + rabbit HRP polymer. Antigen retrieval was performed with heat-induced epitope retrieval

solution (pH 6.2) Diva Decloaker ×20 buffer (Biocare Medical, Concord, CA, USA). The substrates used were Vulcan fast red and 3,3'-diaminobenzidine. Sections were acquired using a Leica DMD108 microscope equipped with appropriate filters and deconvolution software MetaMorph (Leica). The images were analyzed using LAS AF, version 2.2.0, software (Leica Microsystems).

ELISA assays

Cytokine release in supernatant was measured using commercially available ELISA kits for VEGF-A, VEGF-C, Ang1, Ang2, TNF-α, IL-8/CXCL8, and IL-6 (R&D Systems, Minneapolis, MN, USA). The results were normalized for the total protein content in each well. Inhibition of cytokine release is expressed as a percentage of the maximal response, calculated as $(R - R_b)/(R_{max} - R_b) \times 100$, where R is the release in samples treated with the combination of LPS plus CB agonists or antagonists, R_b is the release in unstimulated samples, and R_{max} is the release in samples stimulated with LPS alone.
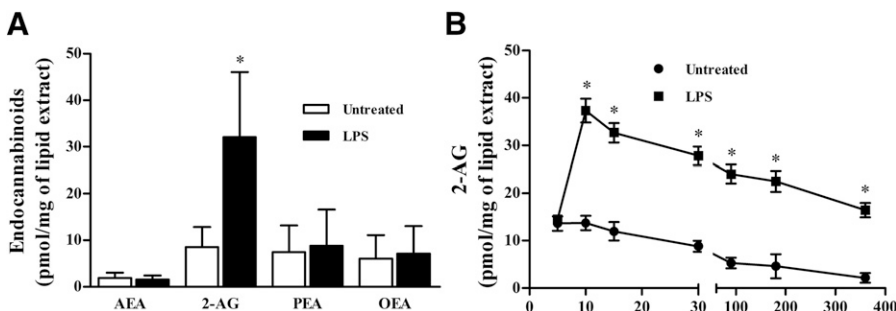
Statistical analysis

The data are expressed as the mean ± SD of the indicated number of experiments. Statistical analysis was performed using Student's *t* test or 1-way ANOVA, followed by Dunnett's test (when comparison was made against a control) or Bonferroni's test (when comparison was made between each pair of groups) using Analyze-it for Microsoft Excel, version 2.16 (Analyze-it Software, Ltd., Leeds, U.K.). Statistically significant differences were accepted when $P \leq 0.05$.
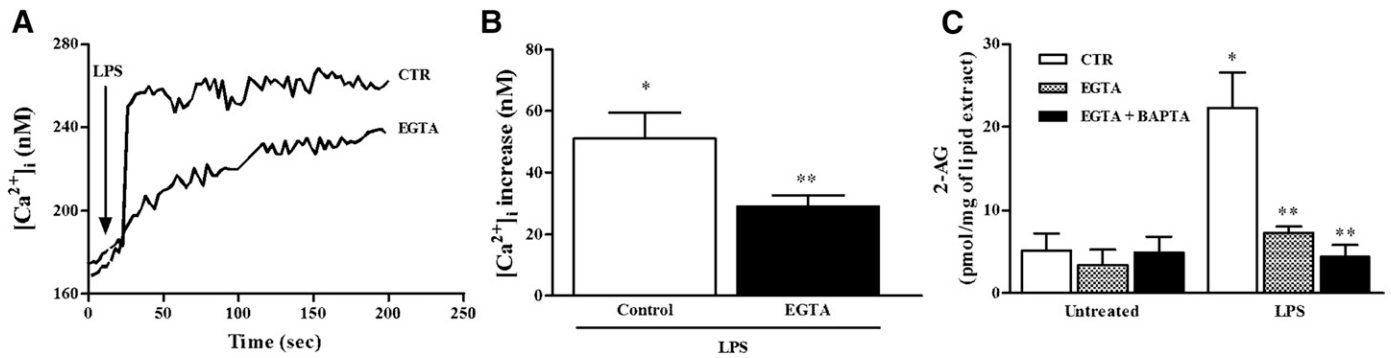
RESULTS

EC production in LPS-activated M2-like HLMs

First, we investigated the phenotype of HLMs by flow cytometry. HLM (identified as $FSc^{hi}SSc^{hi}CD45^+HLA^-DR^+$ cells) homoge-neously expressed CD206 (Supplemental Fig. 1), which might be indicative of an M2-like phenotype [1]. Nevertheless, M2 markers are also expressed by tissue-resident macrophages in an IL-4–independent manner [6].

Next, we evaluated the spontaneous and LPS-induced pro-duction of AEA and 2-AG and of 2 AEA-related mediators, PEA and OEA, which are not CB receptor agonists, by HLMs. HLMs constitutively produced AEA, 2-AG, PEA, and OEA (**Fig. 1A**). In LPS-stimulated HLMs, 2-AG levels peaked after 10 min of stimulation and declined thereafter (Fig. 1B). The production of 2-AG is strictly dependent on the increase in $[Ca^{2+}]i$ [39]. Thus, we monitored $[Ca^{2+}]i$ in LPS-activated HLMs in the absence or presence of the Ca^{2+} chelator EGTA. LPS induced a rapid increase in the $[Ca^{2+}]i$ that was partially prevented by EGTA (1 mM) (**Fig. 2A and B**). This suggests that the LPS-induced $[Ca^{2+}]i$ increase was partially due to the influx of extracellular Ca^{2+}. To functionally link the increase in the $[Ca^{2+}]i$ to the production of
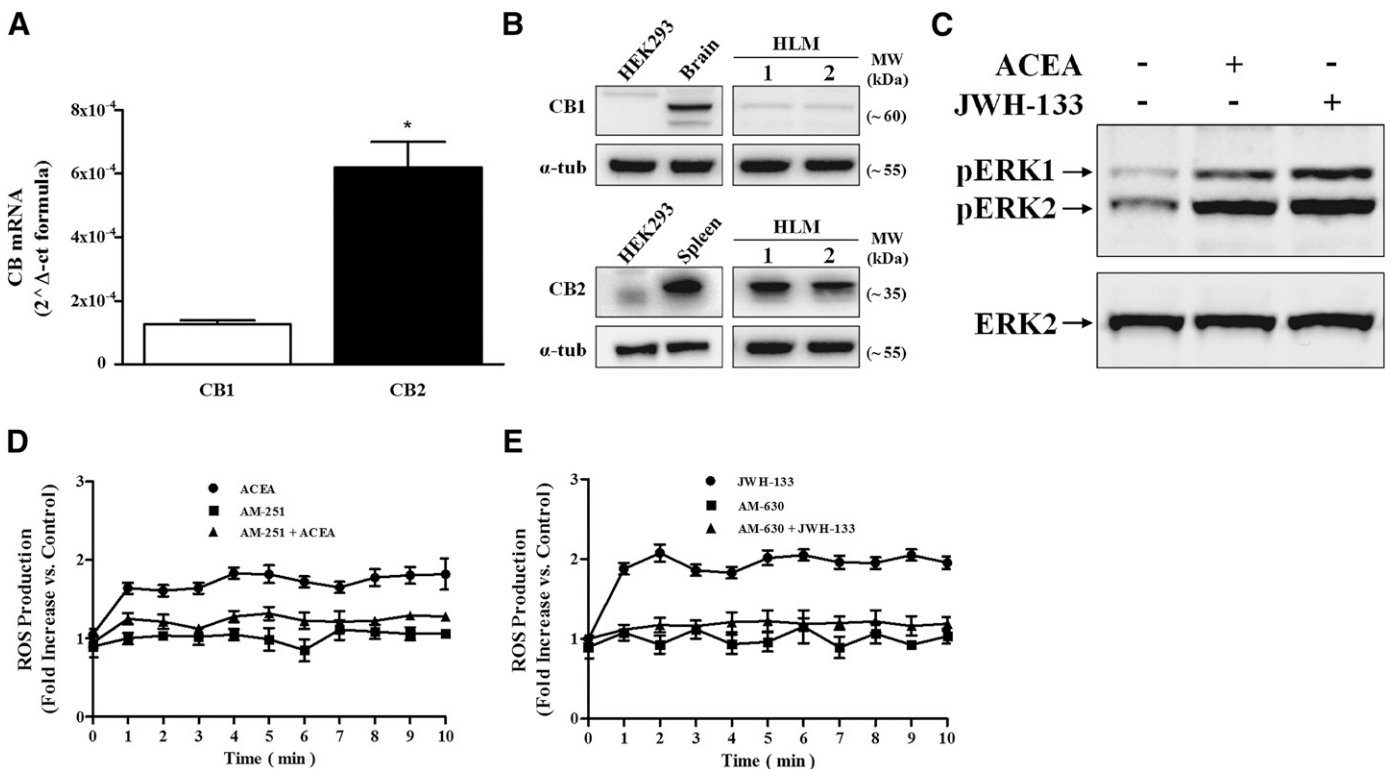

Figure 1. Production of the endocannabinoids AEA, 2-AG and, related mediators, PEA and OEA from untreated (DMSO) and LPS-stimulated HLMs. (A) HLMs were incubated (60 min, 37°C) with or without LPS (1 μg/ml). At the end of incubation, EC levels were evaluated by liquid chromatography-atmospheric pressure chemical ionization-mass spectrometry analysis. Data are mean ± SD of 4 independent experiments. *$P < 0.05$ vs. respective control. (B) Kinetics of LPS-induced 2-AG release from HLMs. Data are mean ± SD of 6 independent experiments with cells from different donors. *$P < 0.05$ vs. respective control (untreated [DMSO]).

Figure 2. Effect of LPS on [Ca²⁺]i. (A) Effect of LPS (1 μg/ml) on $[Ca^{2+}]i$ before and after extracellular Ca^{2+} removal by EGTA (1 mM) in representative HLMs. Each trace is representative of 20 cells recorded in 3 different experiments. (B) Quantification of the effect exerted by LPS on $[Ca^{2+}]i$ in absence or presence of extracellular Ca^{2+}. $*P < 0.05$ vs. untreated, $**P < 0.05$ vs. control. (C) Effect of LPS on 2-AG production after intracellular and extracellular $[Ca^{2+}]$ removal by BAPTA (10 μM) and EGTA (1 mM), respectively. HLMs were pretreated for 5 min with BAPTA and then for 15 min with EGTA before stimulation with LPS (15 min). Data are mean ± SD of 4 independent experiments with cells from different donors. $*P < 0.05$ vs. respective control; $**P < 0.05$ vs. LPS alone.

2-AG induced by LPS, we determined 2-AG levels in HLMs activated with LPS after intracellular and extracellular $[Ca^{2+}]$ removal by BAPTA (10 μM) and EGTA (1 mM), respectively. EGTA almost completely inhibited LPS-induced 2-AG production. The addition of BAPTA to EGTA did not significantly reduce further 2-AG levels (Fig. 2C).

To understand whether the LPS-induced increase in 2-AG levels was due to changes in the expression of EC metabolic enzymes, we next measured the mRNA levels of several 2-AG anabolic and catabolic enzymes after LPS stimulation (90 min, 37°C) of HLMs. LPS did not produce any significant change in the transcriptional levels of the enzymes believed to catalyze 2-AG

Figure 3. HLMs express functional CB₁ and CB₂. (A) CB_1 and CB_2 mRNA expression in HLMs. The results are mean ± SD of 3 different preparations of HLMs. $*P < 0.05$ vs. CB_1 mRNA level. (B) Western blot analysis of CB_1 and CB_2 proteins in 2 representative preparations of HLMs. Negative (HEK-293 cell line) and positive (brain and spleen homogenates for CB_1 and CB_2, respectively) controls are also shown. (C) Western blot analysis of ERK1/2 phosphorylation of HLMs stimulated with ACEA and JWH-133 (30 min, 1 μM). Data are representative of 3 different experiments. (D and E) C2′,7′-dichlorodihydrofluorescein diacetate-labeled HLMs were stimulated with ACEA (D) or JWH-133 (1 μM) (E), and fluorescence was measured for 10 min at 1-min intervals. Cells were pretreated with AM-251 (D) or AM-630 (0.5 μM) (E) for 10 min before stimulation to block CB_1 or CB_2, respectively. Data are mean ± SD of 3 independent experiments with cells from different donors.

TABLE 1. Effects of LPS on the release of VEGF-A, VEGF-C, Ang1, Ang2, TNF-α, IL-6, and IL-8/CXCL8 from HLM

Variable	Untreated	LPS
VEGF-A (pg/mg of protein)	37.2 ± 12.2	105.1 ± 22.5^a
VEGF-C (pg/mg of protein)	165.8 ± 9.7	279.5 ± 26.1^a
Ang1 (pg/mg of protein)	165.3 ± 28.6	390.3 ± 56.3^a
Ang2 (pg/mg of protein)	170.7 ± 47.1	455.6 ± 99.7^a
TNF-α (ng/mg of protein)	1.7 ± 0.6	35.0 ± 5.7^a
IL-6 (ng/mg of protein)	5.9 ± 2.3	63.4 ± 29.1^a
IL-8/CXCL8 (ng/mg of protein)	165.3 ± 59.9	431.0 ± 72.8^a

Data represent the mean $\pm$ SD of 6 independent experiments. $^a P < 0.01$ vs. corresponding value of untreated HLM.

hydrolysis (i.e., MAGL, FAAH-1, ABHD6, and ABHD12 [40]; threshold cycles from 22.51 ± 0.1, 27.21 ± 0.2, 24.0 ± 0.2, and 20.32 ± 0.2 to 22.41 ± 0.09, 27.0 ± 0.1, 24.01 ± 0.02, and 20.22 ± 0.06, respectively). Also, the mRNA levels of the 3 enzymes reported to date to be responsible for 2-AG biosynthesis (DAGLα, DAGLβ, and PLCβ1), did not change (threshold cycles from 24.34 ± 0.2, 23.93 ± 0.1, and 29.62 ± 0.1 to 24.45 ± 0.01, 23.81 ± 0.07, and 29.44 ± 0.18, respectively). These data suggest that the LPS-induced increase of 2-AG might not result from transcriptional changes in the levels of the enzymes responsible for 2-AG biosynthesis and degradation. The 2-AG levels peaked 10 min after stimulation, too short a time for this effect to be due to transcriptional changes.

HLMs express functional CB₁ and CB₂

The production of 2-AG by LPS-activated HLMs prompted us to investigate whether HLMs express a complete EC system. Thus,
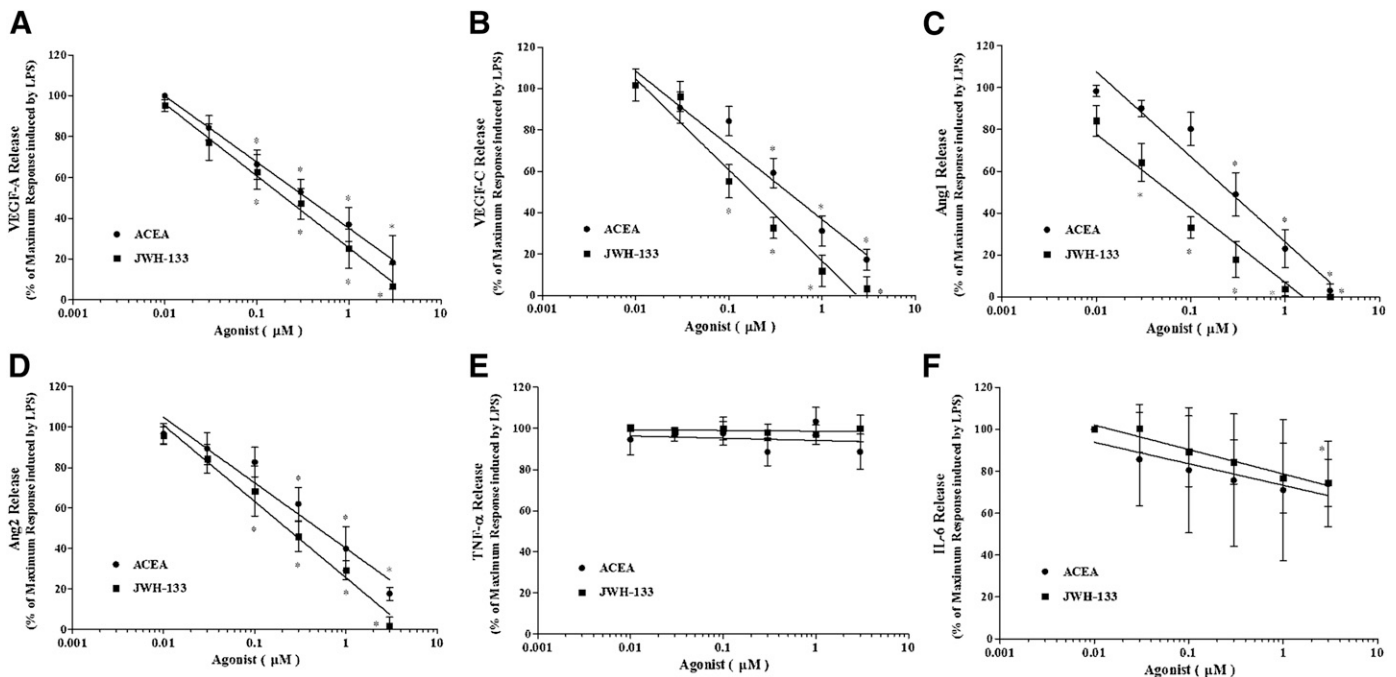
we assessed the constitutive expression of CB₁ and CB₂ in HLMs using quantitative PCR and Western blot. HLMs express CB₁ and CB₂ at the mRNA (**Fig. 3A**) and protein (Fig. 3B) level. LPS stimulation did not modify the expression of either CB₁ or CB₂ mRNA (data not shown), although it might still modulate CB receptor trafficking and surface expression [41].

Activation of both CB₁ and CB₂ induces ERK1/2 phosphorylation [42] and ROS production in mouse macrophages [24]. Thus, we evaluated whether CB₁ and CB₂ agonists could activate ERK1/2 phosphorylation and ROS production in HLMs. Selective agonists of CB₁ (ACEA) and CB₂ (JWH-133) induced phosphorylation of ERK1/2 (Fig. 3C) and ROS production (Fig. 3D and E). Preincubation with either CB₁ (AM-251) (Fig. 3D) or CB₂ (AM-630) (Fig. 3E) antagonists before stimulation with their respective agonists reduced ROS production. Preincubation with the CB₁ antagonist before the CB₂ agonist or with the CB₂ antagonist before the CB₁ agonist did not modify ROS production by the agonists (data not shown).

CB₁ and CB₂ agonists inhibit HLM production of angiogenic and lymphangiogenic factors

We have previously demonstrated that HLMs produce angiogenic (VEGF-A) and lymphangiogenic (VEGF-C) factors [43]. In addition, LPS induces the release of angiopoietins (Ang1 and Ang2), together with VEGFs and cytokines (**Table 1**).

We examined the effects of CB agonists on LPS-induced production of angiogenic and lymphangiogenic factors by HLMs. CB₁ and CB₂ agonists did not modify the spontaneous release of angiogenic and lymphangiogenic factors (Supplemental Table 1). However, ACEA and JWH-133 concentration-dependently

Figure 4. CB receptor activation reduces LPS-induced HLM production of angiogenic and lymphangiogenic factors. (A–E) HLMs were preincubated (20 min, 37°C) with or without the indicated concentrations of ACEA (black circles) or JWH-133 (black squares) and then stimulated (18 h, 37°C) with LPS (1 μg/ml). Data are expressed as the percentage of the maximum response induced by LPS alone for VEGF-A (A), VEGF-C (B), Ang1 (C), Ang2 (D), TNF-α (E), and IL-6 (F). Data are mean $\pm$ SD of 7 independent experiments with cells from different donors. $^*P < 0.05$ vs. maximum response of LPS.

inhibited LPS-induced production of VEGF-A, VEGF-C, Ang1, and Ang2 (**Fig. 4A–D**). The inhibitory effect of the CB_2 agonist JWH-133 on VEGF-A release was comparable to that of the CB_1 agonist ACEA (IC_{50} of ACEA, 316 ± 74 nM vs. IC_{50} of JWH-133, 202 ± 57 nM). In contrast, JWH-133 was more potent than ACEA at inhibiting VEGF-C (IC_{50} of ACEA, 411 ± 42 nM; IC_{50} of JWH-133, 187 ± 36 nM), Ang1 (IC_{50} of ACEA, 269 ± 49 nM; IC_{50} of JWH-133, 61 ± 37 nM), and Ang2 (IC_{50} of ACEA, 496 ± 62 nM; IC_{50} of JWH-133, 213 ± 41 nM) production. The inhibitory effects of ACEA and JWH-133 on VEGF-A, VEGF-C (**Fig. 5**), Ang1 (Supplemental Fig. 3), and Ang2 (data not shown) production from LPS-activated HLMs were completely reversed by preincubation with the CB_1 (AM-251) and CB_2 (AM-630) antagonist, respectively. CB_1 and CB_2 agonists did not modulate LPS-induced production of TNF-α (Fig. 4E) or IL-8/CXCL8 (Supplemental Fig. 2), and IL-6 production was reduced only at the highest concentration of JWH-133 (Fig. 4F).

We evaluated the effects of CB_1 and CB_2 agonists in another model of human macrophages, MDMs. MDMs express CB_1 and CB_2 at the mRNA (**Fig. 6A**) and protein (Fig. 6B) level. ACEA and JWH-133 did not modify the production of VEGF-A in response to LPS (Fig. 6C) nor did they modulate the release of TNF-α (Fig. 6D). Accordingly, CB agonists did not induce ERK1/2 phosphorylation (data not shown).
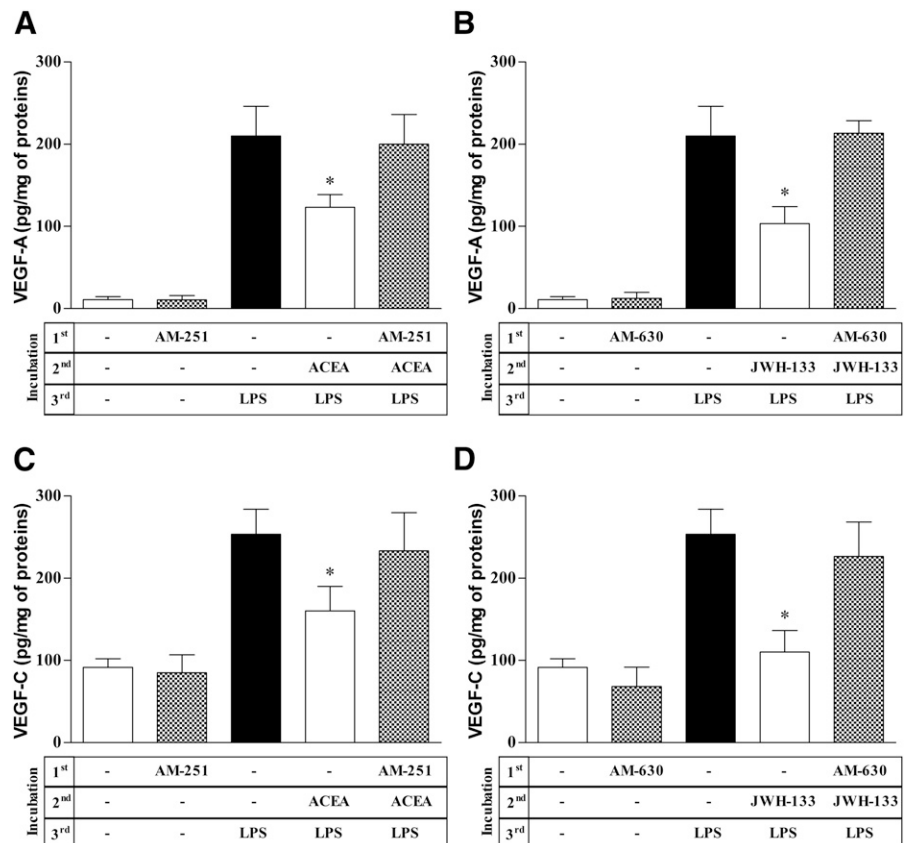
Because LPS induces the production of the endogenous CB agonist 2-AG by HLMs, we questioned whether 2-AG production would modulate the LPS-elicited HLM response. Stimulation of HLMs with LPS in the presence of OMDM-169
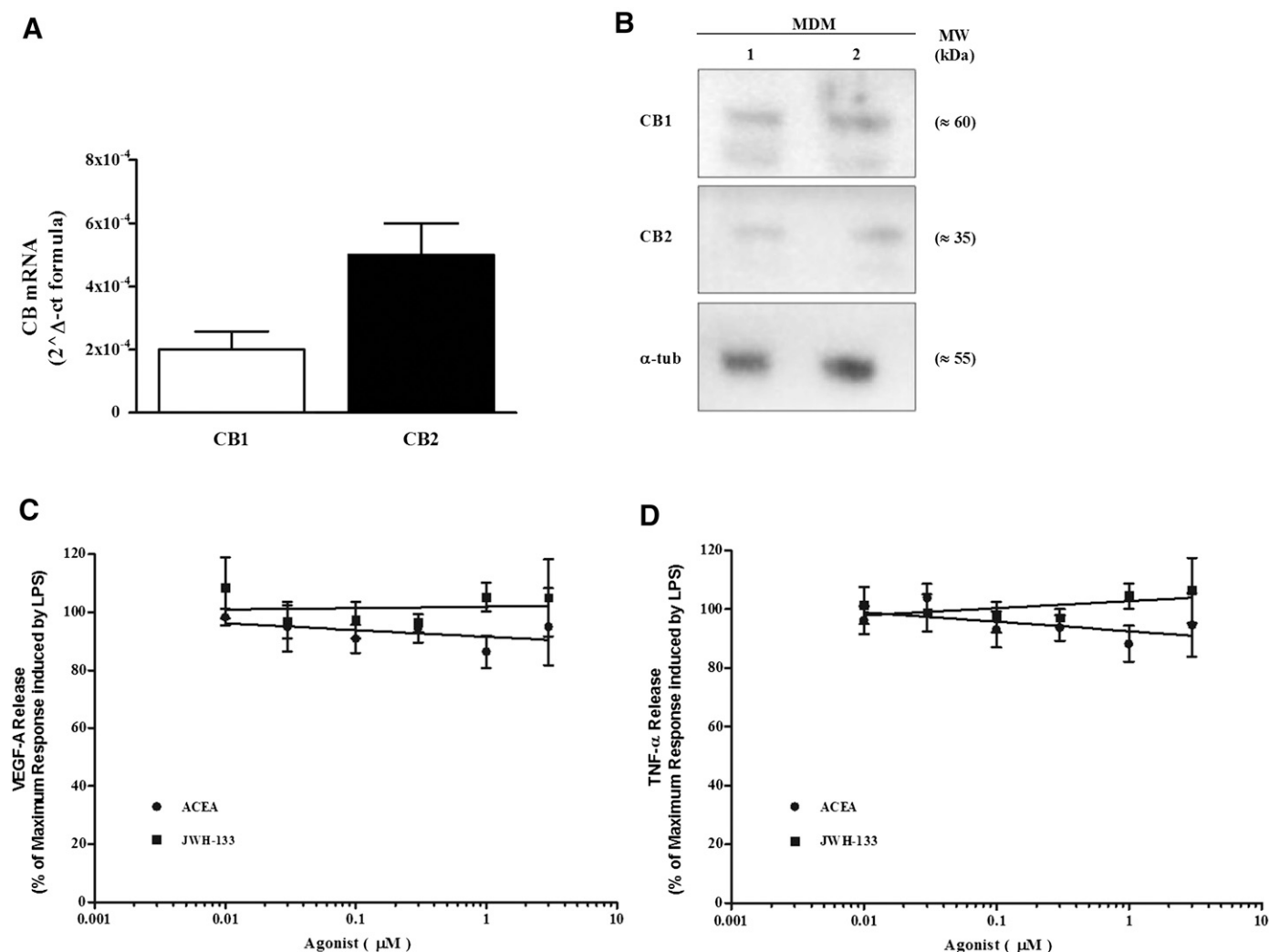
(an inhibitor of 2-AG enzymatic hydrolysis by MAGL) [44] or OMDM-188 (an inhibitor of 2-AG biosynthesis by DAGL) [45] did not modulate VEGF-A (**Fig. 7A**), VEGF-C, angiopoietins, or TNF-α production (data not shown). To verify the effective inhibition of OMDM-169 and OMDM-188, we assessed 2-AG levels in LPS-activated HLMs in the presence of these inhibitors. As expected, OMDM-169 increased (Fig. 7B) and OMDM-188 reduced (Fig. 7C) 2-AG levels in response to LPS.

Expression of CB receptors by lung cancer-associated macrophages

Our results show that activation of CB receptors reduces LPS-elicited production of angiogenic and lymphangiogenic factors by HLMs. Thus, CB receptors might represent therapeutic targets to modulate macrophage-assisted angiogenesis and lymphangiogenesis. Macrophages infiltrate most tumors and contribute to the development of several cancer hallmarks, including angiogenesis [46, 47]. Therefore, we assessed lung cancer-associated macrophage expression of CB receptors by immunohistochemistry using an anti-CD68 antibody to detect macrophages. As a control, we assessed the expression of CB receptors in HLMs from nontumor lung biopsies. Confirming our data (Fig. 3), we identified HLM expression of CB_1 and CB_2 in nontumor tissue (**Fig. 8A**). Also, lung cancer-associated macrophages showed CB_1 and CB_2 expression (Fig. 8A). The specificity of anti-CD68, CB_1, and CB_2 antibodies was assessed by staining human tonsil tissue for CD68 and CB_2 and adrenal tissue for CB_1 (Fig. 8B).

Figure 5. CB receptor antagonists inhibit effects of ACEA and JWH-133 on LPS-induced HLM production of angiogenic and lymphangiogenic factors. (A–D) HLMs were preincubated (10 min, 37°C) with or without AM-251 (0.5 μM) (A and C) or AM-630 (0.5 μM) (B and D), stimulated (20 min, 37°C) with ACEA (0.3 μM) (A and C) or JWH-133 (0.3 μM) (B and D), and finally stimulated (18 h, 37°C) with LPS (1 μg/ml). VEGF-A (A and B) and VEGF-C (C and D) release was determined by ELISA. Data are mean ± SD of 4 independent experiments with cells from different donors. *$P < 0.05$ vs. LPS alone.
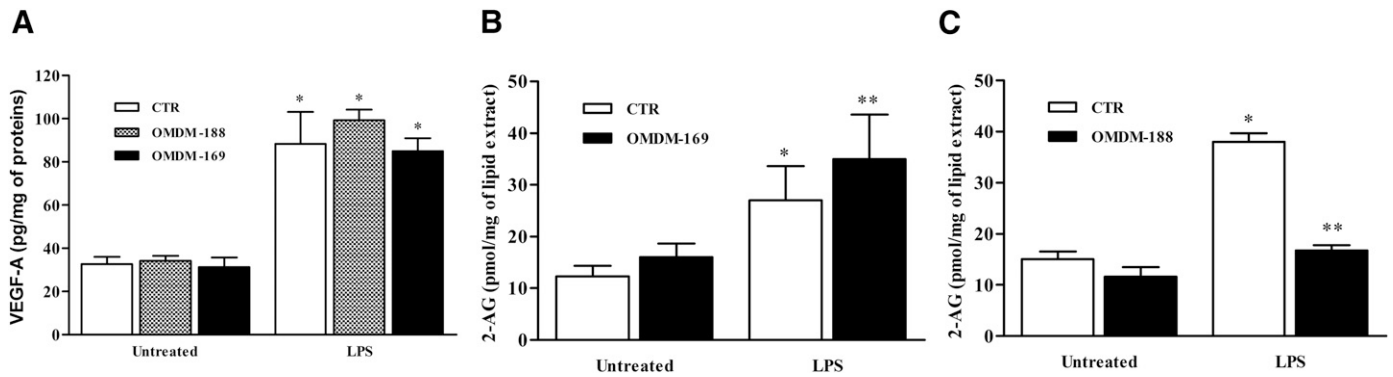
A

B

C

D

Figure 6. Cannabinoid system in MDMs. (A) CB_1 and CB_2 mRNA expression in MDMs. Results are mean ± SD of 3 different preparations of MDMs. *$P < 0.05$ vs. CB_1 mRNA level. (B) Western blot analysis of CB_1 and CB_2 proteins in 2 preparations of MDMs. (C and D) CB receptor activation does not modulate LPS-induced production of VEGF-A and TNF-α. MDMs were preincubated (20 min, 37°C) with or without the indicated concentrations of ACEA (black circles) or JWH-133 (black squares) and stimulated (18 h, 37°C) with LPS (1 μg/ml). Data are expressed as percentage of the maximum response induced by LPS alone for VEGF-A (C) and TNF-α (D). Data are mean ± SD of 4 independent experiments with cells from different donors.

DISCUSSION

In the present study, we have demonstrated that HLMs show a constitutive production of ECs (namely 2-AG) and EC related mediators (OEA and PEA) and the selective LPS-induced production of 2-AG. The latter is dependent on the influx of extracellular Ca^{2+} induced by LPS in HLMs. Moreover, we have demonstrated that isolated HLMs express functional CB_1 and CB_2, as assessed by agonist-induced ERK1/2 phosphorylation and ROS production. CB_1 and CB_2 agonists (ACEA and JWH-133, respectively) reduced the LPS-induced production of angiogenic (VEGF-A) and lymphangiogenic (VEGF-C) factors and angiopoietins (Ang1 and Ang2) from HLMs but not MDMs. The translational relevance of these findings is supported by the observed expression by lung cancer-associated macrophages of CB_1 and CB_2.
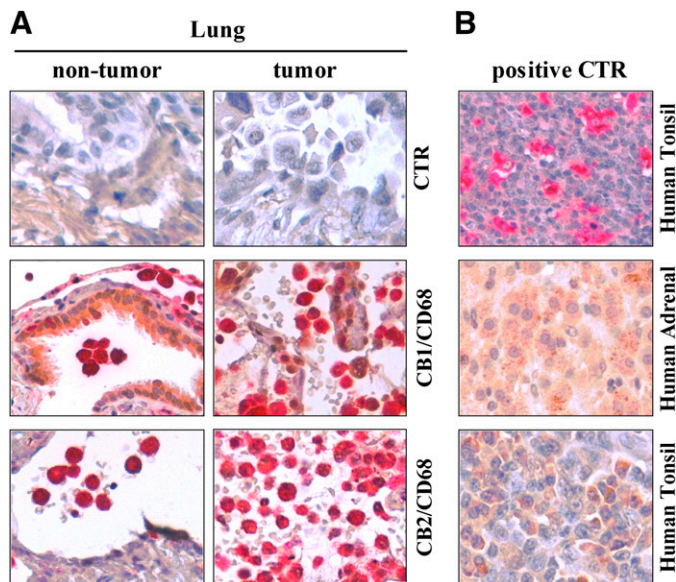
Human macrophages isolated from lungs likely represent a heterogeneous population comprising at least alveolar and interstitial macrophages. In addition, the presence of lung cancer and/or underlying lung disease might influence the biology of HLMs even at distant sites [48]. In our study, we used HLMs isolated only from macroscopically healthy lung tissue. In addition, our HLM preparations homogeneously expressed HLA-DR and CD206. The latter is a marker of IL-4–induced macrophage M2 activation [1]. Nevertheless, markers of M2 polarization could be expressed by tissue-resident macrophages in an IL-4–independent manner [6]. Further studies are required to understand the complex heterogeneity of HLMs and its relevance to lung biology.

HLMs express a complete endocannabinoid system, in that they express CB receptors and spontaneously release of PEA,

Figure 7. Effects of OMDM-169 and OMDM-188 on LPS-activated HLMs. (A) HLMs were preincubated (20 min, 37°C) with or without OMDM-169 and OMDM-188 (5 μM) and stimulated (18 h, 37°C) with LPS (1 μg/ml). Data are expressed as pg of VEGF-A per mg of total protein. Data are mean ± SD of 5 independent experiments with cells from different donors. *$P < 0.05$ vs. respective control. (B and C) Effect of OMDM-169 and OMDM-188 on 2-AG production induced by LPS, respectively. HLMs were preincubated (20 min, 37°C) with or without OMDM-169 and OMDM-188 (5 μM) and stimulated (60 min [B] and 15 min for [C], 37°C) with LPS (1 μg/ml). Data are mean ± SD of 5 independent experiments with cells from different donors. *$P < 0.05$ vs. respective control. **$P < 0.05$ vs. LPS alone.

OEA, and 2-AG. LPS stimulation selectively induces the production of the EC 2-AG, strictly dependent on the increase in $[Ca^{2+}]i$ [39]. Furthermore, LPS induces Ca^{2+} influx and Ca^{2+} release from intracellular stores in rat peritoneal macrophages [49]. In addition, zymosan increased $[Ca^{2+}]i$ in a rat alveolar macrophage cell line [50]. Accordingly, we showed that LPS-stimulated HLMs show a rapid increase in $[Ca^{2+}]i$ that is likely due to both extracellular Ca^{2+} influx and intracellular Ca^{2+} release. Nevertheless, LPS-induced production of 2-AG is dependent on extracellular Ca^{2+}, because it was almost completely abolished by the addition of the Ca^{2+} chelator EGTA.

Figure 8. HLMs and lung cancer-associated macrophages express CB receptors. (A) Sections of nontumor and tumor lung tissue were stained for CD68 (red), CB$_1$, or CB$_2$ (brown). Colocalizations of CD68 and either CB$_1$ or CB$_2$ are identified as red signals with brown dots. (B) Positive control. Specificity of anti-CD68, CB$_1$, and CB$_2$ antibodies was assessed by staining human tonsil tissue for CD68 and CB$_2$ and adrenal tissue for CB$_1$.

Along with evaluating the expression of CB receptors in HLMs, we tested their functionality by assessing agonist-induced ERK1/2 phosphorylation and ROS production. CB agonists induced ERK1/2 phosphorylation and ROS production. The specificity of the latter results was confirmed by the absence of ROS production when HLMs were stimulated with CB agonists in the presence of their respective antagonists. In partial disagreement with our results, it was recently reported that only the activation of CB$_1$ induces ROS production [24]. These discrepancies could very well be explained by differences in the cell types used (HLMs vs. the murine macrophage cell line RAW264.7) and CB$_2$ agonists used (JWH-133 vs. JWH-015). Further studies are required to dissect the complexity of signaling events induced by CB receptor activation in different cell subsets.

CB agonists markedly reduce LPS-activated production of angiogenic and lymphangiogenic factors and angiopoietins. However, they do not modulate TNF-α and IL-8/CXCL8 production. Also, the production of IL-6 was reduced only at the highest concentration of JWH-133. The anti-inflammatory effect of ECs and CB agonists has been demonstrated in several in vitro and in vivo models [17]. Although our data do not support a modulation of classic proinflammatory cytokines and chemokines (i.e., TNF-α, IL-8/CXCL8, and IL-6) by CB agonists in LPS-activated HLMs, the reduction of angiogenic and lymphangiogenic factors could still have a remarkable effect on the inflammatory condition associated with macrophage-assisted vascular remodeling (i.e., cancer) [2–4]. Instead, the production of VEGF-A induced by LPS in MDM was not modulated by CB agonists. Accordingly, MDMs express CB receptors that are not functional, as assessed by the absence of CB agonist-induced ERK1/2 phosphorylation. The differences between the data obtained with HLMs and MDMs can be explained by the different ontogeny of in vitro-derived macrophages (i.e., MDMs) and tissue-resident macrophages (i.e., HLMs) [9, 51]. Furthermore, evidence has shown that tissue-derived factors modulate macrophage function [6–8, 52–54]. It will be interesting to investigate whether lung tissue-derived signals modulate macrophage responsiveness to CB receptor activation and the relevance of the latter to lung pathophysiology.

Because LPS induces the production of the endogenous CB agonist 2-AG and CB agonists modulate the LPS-induced HLM response, we speculated that 2-AG could participate in LPS-elicited HLM production of angiogenic and lymphangiogenic factors and angiopoietins. To address this question we used an inhibitor of 2-AG enzymatic hydrolysis (OMDM-169) [44] and an inhibitor of 2-AG biosynthesis (OMDM-188) [45]. We confirmed that OMDM-169 and OMDM-188 increase and reduce LPS-elicited 2-AG production, respectively. However, stimulation of HLMs with LPS in the presence of these inhibitors did not modulate VEGF-A, VEGF-C, angiopoietin, or TNF-α production. Nonetheless, LPS-induced 2-AG production might affect other aspects of macrophage biology not tested in our experimental model.

Macrophage-assisted vascular remodeling plays a central role in chronic inflammation and tumor growth [2–4]. CB activation reduces angiogenesis in several in vitro and in vivo models [28–32]. In addition, CB receptors have been proposed as therapeutic targets for the inhibition of lung cancer growth and metastasis [32, 55]. Because we found that CB agonists inhibit LPS-induced HLM production of angiogenic factors and also that lung cancer-associated macrophages express CB receptors, it will be interesting to assess whether CB receptor activation modulates tumor vascularization via reduction of macrophage-derived angiogenic and lymphangiogenic factors. The answer to this question is likely to provide relevant information for defining CB receptors as novel targets to modulate macrophage-assisted vascular remodeling in cancer and chronic inflammation.

AUTHORSHIP

R.I.S., S.L., F.B., V.D., A.F., M.S., G.M. participated in research design. R.I.S., S.L., F.B., A.S., G.V., F.A.I., P.O., F.P., M.T.L. conducted experiments. R.I.S., S.L., P.O., F.G., M.T.L. performed data analysis. R.I.S., S.L., F.B., F.A.I., G.M., V.D. wrote or contributed to the writing the manuscript.

ACKNOWLEDGMENTS

DISCLOSURES

The authors declare no conflicts of interest.

REFERENCES

1. Sica, A., Mantovani, A. (2012) Macrophage plasticity and polarization: in vivo veritas. *J. Clin. Invest.* **122,** 787–795.
2. Dirkx, A. E., Oude Egbrink, M. G., Wagstaff, J., Griffioen, A. W. (2006) Monocyte/macrophage infiltration in tumors: modulators of angiogenesis. *J. Leukoc. Biol.* **80,** 1183–1196.
3. Solinas, G., Germano, G., Mantovani, A., Allavena, P. (2009) Tumor-associated macrophages (TAM) as major players of the cancer-related inflammation. *J. Leukoc. Biol.* **86,** 1065–1073.
4. Squadrito, M. L., De Palma, M. (2011) Macrophage regulation of tumor angiogenesis: implications for cancer therapy. *Mol. Aspects Med.* **32,** 123–145.
5. Xue, J., Schmidt, S. V., Sander, J., Draffehn, A., Krebs, W., Quester, I., De Nardo, D., Gohel, T. D., Emde, M., Schmidleithner, L., Ganesan, H., Nino-Castro, A., Mallmann, M. R., Labzin, L., Theis, H., Kraut, M., Beyer, M., Latz, E., Freeman, T. C., Ulas, T., Schultze, J. L. (2014) Transcriptome-based network analysis reveals a spectrum model of human macrophage activation. *Immunity* **40,** 274–288.
6. Okabe, Y., Medzhitov, R. (2014) Tissue-specific signals control reversible program of localization and functional polarization of macrophages. *Cell* **157,** 832–844.
7. Haldar, M., Kohyama, M., So, A. Y., Kc, W., Wu, X., Briseño, C. G., Satpathy, A. T., Kretzer, N. M., Arase, H., Rajasekaran, N. S., Wang, L., Egawa, T., Igarashi, K., Baltimore, D., Murphy, T. L., Murphy, K. M. (2014) Heme-mediated SPI-C induction promotes monocyte differentiation into iron-recycling macrophages. *Cell* **156,** 1223–1234.
8. Schneider, C., Nobs, S. P., Kurrer, M., Rehrauer, H., Thiele, C., Kopf, M. (2014) Induction of the nuclear receptor PPAR-γ by the cytokine GM-CSF is critical for the differentiation of fetal monocytes into alveolar macrophages. *Nat. Immunol.* **15,** 1026–1037.
9. Ginhoux, F., Jung, S. (2014) Monocytes and macrophages: developmental pathways and tissue homeostasis. *Nat. Rev. Immunol.* **14,** 392–404.
10. Guilliams, M., De Kleer, I., Henri, S., Post, S., Vanhoutte, L., De Prijck, S., Deswarte, K., Malissen, B., Hammad, H., Lambrecht, B. N. (2013) Alveolar macrophages develop from fetal monocytes that differentiate into long-lived cells in the first week of life via GM-CSF. *J. Exp. Med.* **210,** 1977–1992.
11. Matsuda, L. A., Lolait, S. J., Brownstein, M. J., Young, A. C., Bonner, T. I. (1990) Structure of a cannabinoid receptor and functional expression of the cloned cDNA. *Nature* **346,** 561–564.
12. Munro, S., Thomas, K. L., Abu-Shaar, M. (1993) Molecular characterization of a peripheral receptor for cannabinoids. *Nature* **365,** 61–65.
13. Di Marzo, V. (2011) Endocannabinoid signaling in the brain: biosynthetic mechanisms in the limelight. *Nat. Neurosci.* **14,** 9–15.
14. Cota, D. (2007) CB1 receptors: emerging evidence for central and peripheral mechanisms that regulate energy balance, metabolism, and cardiovascular health. *Diabetes Metab. Res. Rev.* **23,** 507–517.
15. Kaplan, B. L. (2013) The role of CB1 in immune modulation by cannabinoids. *Pharmacol. Ther.* **137,** 365–374.
16. Klein, T. W., Newton, C., Larsen, K., Lu, L., Perkins, I., Nong, L., Friedman, H. (2003) The cannabinoid system and immune modulation. *J. Leukoc. Biol.* **74,** 486–496.
17. Turcotte, C., Chouinard, F., Lefebvre, J. S., Flamand, N. (2015) Regulation of inflammation by cannabinoids, the endocannabinoids 2-arachidonoyl-glycerol and arachidonoyl-ethanolamine, and their metabolites. *J. Leukoc. Biol.* **97,** 1049–1070.
18. Atwood, B. K., Mackie, K. (2010) CB2: a cannabinoid receptor with an identity crisis. *Br. J. Pharmacol.* **160,** 467–479.
19. Louvet, A., Teixeira-Clerc, F., Chobert, M. N., Deveaux, V., Pavoine, C., Zimmer, A., Pecker, F., Mallat, A., Lotersztajn, S. (2011) Cannabinoid CB2 receptors protect against alcoholic liver disease by regulating Kupffer cell polarization in mice. *Hepatology* **54,** 1217–1226.
20. Romano, B., Borrelli, F., Fasolino, I., Capasso, R., Piscitelli, F., Cascio, M., Pertwee, R., Coppola, D., Vassallo, L., Orlando, P., Di Marzo, V., Izzo, A. (2013) The cannabinoid TRPA1 agonist cannabichromene inhibits nitric oxide production in macrophages and ameliorates murine colitis. *Br. J. Pharmacol.* **169,** 213–229.
21. Montecucco, F., Burger, F., Mach, F., Steffens, S. (2008) CB2 cannabinoid receptor agonist JWH-015 modulates human monocyte migration through defined intracellular signaling pathways. *Am. J. Physiol. Heart Circ. Physiol.* **294,** H1145–H1155.
22. Rom, S., Zuluaga-Ramirez, V., Dykstra, H., Reichenbach, N. L., Pacher, P., Persidsky, Y. (2013) Selective activation of cannabinoid receptor 2 in leukocytes suppresses their engagement of the brain endothelium and protects the blood-brain barrier. *Am. J. Pathol.* **183,** 1548–1558.
23. Jourdan, T., Godlewski, G., Cinar, R., Bertola, A., Szanda, G., Liu, J., Tam, J., Han, T., Mukhopadhyay, B., Skarulis, M. C., Ju, C., Aouadi, M., Czech, M. P., Kunos, G. (2013) Activation of the Nlrp3 inflammasome in infiltrating macrophages by endocannabinoids mediates beta cell loss in type 2 diabetes. *Nat. Med.* **19,** 1132–1140.
24. Han, K. H., Lim, S., Ryu, J., Lee, C. W., Kim, Y., Kang, J. H., Kang, S. S., Ahn, Y. K., Park, C. S., Kim, J. J. (2009) CB1 and CB2 cannabinoid receptors differentially regulate the production of reactive oxygen species by macrophages. *Cardiovasc. Res.* **84,** 378–386.
25. Sugawara, K., Bíró, T., Tsuruta, D., Toth, B. I., Kromminga, A., Zakany, N., Zimmer, A., Funk, W., Gibbs B. F., Zimmer A., Paus R. (2012) Endocannabinoids limit excessive mast cell maturation and activation in human skin. *J. Allergy Clin. Immunol.* **129,** 726.e728–738.e728.

26. Sugawara, K., Zákány, N., Hundt, T., Emelianov, V., Tsuruta, D., Schäfer, C., Kloepper, J. E., Bíró, T., Paus, R. (2013) Cannabinoid receptor 1 controls human mucosal-type mast cell degranulation and maturation in situ. *J. Allergy Clin. Immunol.* **132,** 182–193.

27. Marone, G., Granata, F., eds. (2014) *Angiogenesis, Lymphangiogenesis and Clinical Implications.* Karger, Basel.

28. Blázquez, C., Casanova, M. L., Planas, A., Gómez Del Pulgar, T., Villanueva, C., Fernández-Aceñero, M. J., Aragonés, J., Huffman, J. W., Jorcano, J. L., Guzmán, M. (2003) Inhibition of tumor angiogenesis by cannabinoids. *FASEB J.* **17,** 529–531.

29. Casanova, M. L., Blázquez, C., Martínez-Palacio, J., Villanueva, C., Fernández-Aceñero, M. J., Huffman, J. W., Jorcano, J. L., Guzmán, M. (2003) Inhibition of skin tumor growth and angiogenesis in vivo by activation of cannabinoid receptors. *J. Clin. Invest.* **111,** 43–50.

30. De Filippis, D., Russo, A., D'Amico, A., Esposito, G., Pietropaolo, C., Cinelli, M., Russo, G., Iuvone, T. (2008) Cannabinoids reduce granuloma-associated angiogenesis in rats by controlling transcription and expression of mast cell protease-5. *Br. J. Pharmacol.* **154,** 1672–1679.

31. Pisanti, S., Borselli, C., Oliviero, O., Laezza, C., Gazzerro, P., Bifulco, M. (2007) Antiangiogenic activity of the endocannabinoid anandamide: correlation to its tumor-suppressor efficacy. *J. Cell. Physiol.* **211,** 495–503.

32. Portella, G., Laezza, C., Laccetti, P., De Petrocellis, L., Di Marzo, V., Bifulco, M. (2003) Inhibitory effects of cannabinoid CB1 receptor stimulation on tumor growth and metastatic spreading: actions on signals involved in angiogenesis and metastasis. *FASEB J.* **17,** 1771–1773.

33. Blázquez, C., González-Feria, L., Alvarez, L., Haro, A., Casanova, M. L., Guzmán, M. (2004) Cannabinoids inhibit the vascular endothelial growth factor pathway in gliomas. *Cancer Res.* **64,** 5617–5623.

34. Triggiani, M., Granata, F., Petraroli, A., Loffredo, S., Frattini, A., Staiano, R. I., Monaco, G., Marone, G. (2009) Inhibition of secretory phospholipase A2-induced cytokine production in human lung macrophages by budesonide. *Int. Arch. Allergy Immunol.* **150,** 144–155.

35. Matias, I., Petrosino, S., Racioppi, A., Capasso, R., Izzo, A. A., Di Marzo, V. (2008) Dysregulation of peripheral endocannabinoid levels in hyperglycemia and obesity: effect of high fat diets. *Mol. Cell. Endocrinol.* **286** (Suppl 1), S66–S78.

36. Piscitelli, F., Carta, G., Bisogno, T., Murru, E., Cordeddu, L., Berge, K., Tandy, S., Cohn, J. S., Griinari, M., Banni, S., Di Marzo, V. (2011) Effect of dietary krill oil supplementation on the endocannabinoidome of metabolically relevant tissues from high-fat-fed mice. *Nutr. Metab. (Lond)* **8,** 51.

37. Secondo, A., Staiano, R. I., Scorziello, A., Sirabella, R., Boscia, F., Adornetto, A., Valsecchi, V., Molinaro, P., Canzoniero, L. M., Di Renzo, G., Annunziato, L. (2007) BHK cells transfected with NCX3 are more resistant to hypoxia followed by reoxygenation than those transfected with NCX1 and NCX2: possible relationship with mitochondrial membrane potential. *Cell Calcium* **42,** 521–535.

38. Grynkiewicz, G., Poenie, M., Tsien, R. Y. (1985) A new generation of Ca2 + indicators with greatly improved fluorescence properties. *J. Biol. Chem.* **260,** 3440–3450.

39. Zhang, L., Wang, M., Bisogno, T., Di Marzo, V., Alger, B. E. (2011) Endocannabinoids generated by Ca2+ or by metabotropic glutamate receptors appear to arise from different pools of diacylglycerol lipase. *PLoS One* **6,** e16305.

40. Alhouayek, M., Masquelier, J., Muccioli, G. G. (2014) Controlling 2-arachidonoylglycerol metabolism as an anti-inflammatory strategy. *Drug Discov. Today* **19,** 295–304.

41. Kleyer, J., Nicolussi, S., Taylor, P., Simonelli, D., Furger, E., Anderle, P., Gertsch, J. (2012) Cannabinoid receptor trafficking in peripheral cells is dynamically regulated by a binary biochemical switch. *Biochem. Pharmacol.* **83,** 1393–1412.

42. Bosier, B., Muccioli, G. G., Hermans, E., Lambert, D. M. (2010) Functionally selective cannabinoid receptor signalling: therapeutic implications and opportunities. *Biochem. Pharmacol.* **80,** 1–12.

43. Granata, F., Frattini, A., Loffredo, S., Staiano, R. I., Petraroli, A., Ribatti, D., Oslund, R., Gelb, M. H., Lambeau, G., Marone, G., Triggiani, M. (2010) Production of vascular endothelial growth factors from human lung macrophages induced by group IIA and group X secreted phospholipases A2. *J. Immunol.* **184,** 5232–5241.

44. Bisogno, T., Ortar, G., Petrosino, S., Morera, E., Palazzo, E., Nalli, M., Maione, S., Di Marzo, V.; Endocannabinoid Research Group. (2009) Development of a potent inhibitor of 2-arachidonoylglycerol hydrolysis with antinociceptive activity in vivo. *Biochim. Biophys. Acta* **1791,** 53–60.

45. Ortar, G., Bisogno, T., Ligresti, A., Morera, E., Nalli, M., Di Marzo, V. (2008) Tetrahydrolipstatin analogues as modulators of endocannabinoid 2-arachidonoylglycerol metabolism. *J. Med. Chem.* **51,** 6970–6979.

46. De Palma, M., Lewis, C. E. (2013) Macrophage regulation of tumor responses to anticancer therapies. *Cancer Cell* **23,** 277–286.

47. Galdiero, M. R., Garlanda, C., Jaillon, S., Marone, G., Mantovani, A. (2013) Tumor associated macrophages and neutrophils in tumor progression. *J. Cell. Physiol.* **228,** 1404–1412.

48. Hussell, T., Bell, T. J. (2014) Alveolar macrophages: plasticity in a tissue-specific context. *Nat. Rev. Immunol.* **14,** 81–93.

49. Zhou, X., Yang, W., Li, J. (2006) Ca2+- and protein kinase C-dependent signaling pathway for nuclear factor-kappaB activation, inducible nitric-oxide synthase expression, and tumor necrosis factor-alpha production in lipopolysaccharide-stimulated rat peritoneal macrophages. *J. Biol. Chem.* **281,** 31337–31347.

50. Castro, R., Sun, X. H., Liu, X. B., Martinez, J. R., Zhang, G. H. (2008) Inhibition of Ca2+ influx by surfactant in NR8383 alveolar macrophages. *Inflamm. Res.* **57,** 489–496.

51. Gomez Perdiguero, E., Geissmann, F. (2013) Myb-independent macrophages: a family of cells that develops with their tissue of residence and is involved in its homeostasis. *Cold Spring Harb. Symp. Quant. Biol.* **78,** 91–100.

52. Bain, C. C., Bravo-Blas, A., Scott, C. L., Gomez Perdiguero, E., Geissmann, F., Henri, S., Malissen, B., Osborne, L. C., Artis, D., Mowat, A. M. (2014) Constant replenishment from circulating monocytes maintains the macrophage pool in the intestine of adult mice. *Nat. Immunol.* **15,** 929–937.

53. Gautier, E. L., Ivanov, S., Williams, J. W., Huang, S. C., Marcelin, G., Fairfax, K., Wang, P. L., Francis, J. S., Leone, P., Wilson, D. B., Artyomov, M. N., Pearce, E. J., Randolph, G. J. (2014) Gata6 regulates aspartoacylase expression in resident peritoneal macrophages and controls their survival. *J. Exp. Med.* **211,** 1525–1531.

54. Rosas, M., Davies, L. C., Giles, P. J., Liao, C. T., Kharfan, B., Stone, T. C., O'Donnell, V. B., Fraser, D. J., Jones, S. A., Taylor, P. R. (2014) The transcription factor Gata6 links tissue macrophage phenotype and proliferative renewal. *Science* **344,** 645–648.

55. Preet, A., Qamri, Z., Nasser, M. W., Prasad, A., Shilo, K., Zou, X., Groopman, J. E., Ganju, R. K. (2011) Cannabinoid receptors, CB1 and CB2, as novel targets for inhibition of non-small cell lung cancer growth and metastasis. *Cancer Prev. Res. (Phila.)* **4,** 65–75.